Hydroxyl radicals and hydrogen peroxide formation at non-thermal plasma-water interface

Yi Yi Zhao, Tao Wang, Scott J. MacGregor, Qing Chun Ren, Mark P. Wilson, Igor V. Timoshkin

Abstract—This work investigated hydroxyl radicals and hydrogen peroxide formation under a needle-plate electrode configuration using positive-polarity d.c. discharges generated in air, nitrogen and helium. The discharge mode in air and nitrogen was found to change above ultrapure water, initially a nanosecond pulse discharge was observed, transitioning to a diffuse discharge due to the increasing conductivity of the water. The discharge in helium was a nanosecond pulse discharge and the repetition rate increased with increasing water conductivity. It was found that hydroxyl radicals contribute to 7%, 78% and 70% of hydrogen peroxide formation when using ultrapure water in air, nitrogen and helium, respectively. It is suggested that hydroxyl radicals are formed by water reactions with energetic positive ions and neutral particles such as N_2^+, He^+, O, H and HO_2. Part of the hydrogen peroxide is formed directly from atoms and radical reactions with water in nitrogen and helium, while oxygen reactions are heavily involved for hydrogen peroxide formation in air. A fluorophotometry method, using terephthalic acid, was used to directly quantify the formation of hydroxyl radicals and compared with the tert-butanol method.

Index Terms—Hydroxyl radical, Hydrogen peroxide, Non-thermal plasma, Liquid electrode, Diffuse discharge.

I. Introduction

Advanced oxidation processes (AOPs) using O_3, H_2O_2, UV, or Fenton reactions have shown potential in treating hard-degradable and toxic organic compounds in wastewater [1, 2]. Hydroxyl radicals (OH) produced in AOPs have high oxidation ability and the reactions do not produce carcinogenic by-products [3]; they can react with substances in a non-selective manner and convert organic compounds into carbon dioxide and water. The general hydroxyl radical reaction constant is more than 10^9 $M^{-1}s^{-1}$ [4]. Hydroxyl radicals are also an important source of H_2O_2 formation. As an alternative to traditional AOPs, non-thermal plasma induced AOPs have been extensively investigated over the last 30 years. The reactions occurring at the plasma-water interface lead to chemical activations by producing active species in-situ, including ions, reactive radicals, excited molecules and atoms, without the requirement for additional chemicals [5]. Hydrogen peroxide has been considered as a useful, but not perfect, indicator of OH radicals in plasma systems [6]; it is believed to be the major product of OH radical dimerization reactions [6, 7].

Non-thermal plasma discharges with at least one water electrode have been extensively investigated. P. Andre [8] investigated diffuse discharges between two, non-metallic, liquid electrodes and characterised the plasma state in the inter-electrode gap under d.c. voltage. X. Lu [9, 10] studied the ignition of discharges between metal and water electrodes using an a.c. power supply and investigated the spatial and temporal behavior of OH emission to resolve the relative OH concentration during the discharge. Kanazawa found an OH radical production rate of the order of 10^{-9} Ms^{-1} using pulsed surface streamer discharges [11]; and of the order of 10^{-8} Ms^{-1} using plasma jets [12]. Various methods have been employed for OH radical measurement, such as spectrophotometry [13], high-performance liquid chromatography (HPLC) [14], fluorophotometry [15], and electron spin resonance (ESR) [16]. Spectrophotometry, using potassium titanium (IV) oxalate ($K_2TiO(C_2O_4)_2{\cdot}2H_2O$), has been used to identify H_2O_2 concentration in a liquid [17]. Tert-butanol has been used as an effective scavenger of OH radicals [18-19].

In the present study, a pin-plate configured discharge reactor was developed to investigate the plasma-water interfacial reactions. The main objectives of this research were to: (1) quantify the OH radical formation at the plasma-water interface during discharge in different gases; (2) validate the hydroxyl radical formation using fluorophotometry and the terephthalic acid method; (3) quantify the H_2O_2 formation by using spectrophotometry and potassium titanium (IV) oxalate; and (4) investigate the reaction paths of OH radicals and H_2O_2 formation.

II. Experimental Processes

A. Reactor design and experimental set-up

The reactor used in the study, shown in Fig. 1(a), has a typical pin-plate electrode configuration, consisting of a 70-mm-high PTFE cylinder, with inner diameter of 40 mm and outer diameter of 50 mm. Two nylon flanges of 100 mm diameter and 10 mm depth were placed at either end of the cylinder, with an 8-mm-diameter copper electrode positioned in the center. A stainless-steel needle with 0.3-mm tip diameter was attached to the high-voltage (HV) electrode. The discharge gap between the needle tip and the solution surface was fixed at 1 mm. The HV electrode was energized with positive-polarity d.c. voltage. For each treatment, a solution of total volume

This paper is submitted for review on 30/12/2015.

All the authors are with the department of electronic and electrical engineering, University of Strathclyde, Royal College Building, 204 George Street, Glasgow, UK, G1 1XW (email: y.zhao@strath.ac.uk, tao.wang@strath.ac.uk)

10 ml was introduced into the reactor via a 5-ml pipette (P5000G, Gilson). Since various gases (air, nitrogen and helium) were used, the sealed reactor was evacuated to a standard pressure of 13 Torr using an Edwards E2M80 rotary-vane vacuum pump, before being refilled with the working gas to atmospheric pressure. This process was repeated twice before each treatment. A conductivity meter (Thermo Orion Star) was employed to measure the conductivity of the solution before and after each treatment.

A Glassman, PS/EJ20R30 power supply was used to provide positive-polarity d.c. voltage. A 6-MΩ current-limiting resistor was connected in series with the reactor to minimize the charging current during the gas discharge. A Tektronix P6015A high-voltage probe with a bandwidth of 75 MHz was employed to measure the voltage applied to the reactor. A 50-Ω coaxial cable was connected to the grounded electrode of the reactor to measure the current waveform. A LeCroy digital oscilloscope (Waverunner 610Zi), with a bandwidth of 1 GHz and sampling rate of 20 GS/s, was used to record the waveforms. A fluorescence spectrophotometer (RF5301PC, Shimadzu Scientific Instruments) was employed to measure the concentration of 2-hydroxyterephthalic acid (HTA), the product of the reaction of OH radicals with terephthalic acid, to determine the concentration of OH radicals produced. When HTA molecules are irradiated with UV light with central wavelength of 310 nm, visible light of wavelength 425 nm is emitted. Also, a spectrophotometer (Thermo Scientific, Evolution 201) was used to measure the concentration of H_2O_2 by measuring the absorption of Titanium (IV) - peroxide complex at the wavelength of 396 nm.

B. Sample preparation and measurement

All solutions were prepared from ultrapure water (Milli-Q type 1 ultrapure water). 200-mg of sodium hydroxide (ACS reagent, ≥97.0%, pellets, Sigma-Aldrich) was weighed and dissolved in 1000 ml of water to make a 5 mM sodium-hydroxide solution. As terephthalic acid only dissolves in alkaline conditions, 332 mg terephthalic acid (98%, Aldrich) was weighed and dissolved in the 1000 ml, 5 mM sodium hydroxide solution, and the solution was left to stand for two hours for complete dissolution. A calibration curve was plotted using 2-hydroxyterephthalic acid (97%, Aldrich) made up with sodium-hydroxide solution to determine the amount of OH radicals.

35.4 g of potassium titanium (IV) oxalate (Technical, ≥90%, Ti basis), $K_2TiO(C_2O_4)_2 \cdot 2H_2O$, was dissolved in 300 ml of ultrapure water. 272 ml of concentrated sulphuric acid (ACS reagent, 95.0%, Aldrich) was mixed with potassium titanium oxalate solution (cooling and care are required) and made up to 1 L with ultrapure water. 20 ml tert-butanol (ACS reagent, ≥99.7%, Aldrich) was mixed in 1 L of ultrapure water to prepare a 0.2 M tert-butanol solution. After treatment, the 5 ml treated sample and 5 ml of titanium reagent were pipetted into a 25 ml volumetric flask and made up to 25 ml with ultrapure water. The molar absorptivity of the titanium (IV)-peroxide complex was measured as $\varepsilon_{396} = 905$ $mol^{-1}cm^{-1}$. Experiments were conducted with treatment times of 5, 10, 15 and 20 minutes, in air, nitrogen and helium under positive-polarity d.c. voltage; each treatment was repeated 3 times.

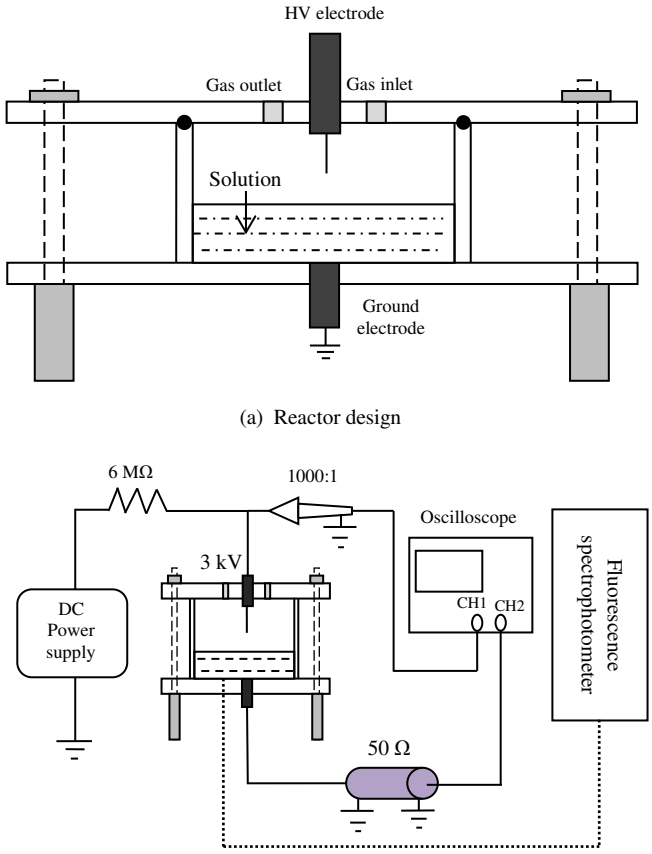

Fig. 1. (a) Schematic diagram of reactor design and (b) experimental set-up.

III. Voltage and Current Characteristics

A. Discharge above ultrapure water

Fig. 2(a), (b), and (c) show the discharge voltage and current waveforms recorded during a discharge in air, using ultrapure water with a conductivity of 0.5 μScm^{-1}. A capacitive current pulse of full width half maximum (FWHM) 17 ns was recorded at the start of the discharge, with a repetition rate of 2×10^5 pulses per second (pps) and a voltage drop of 200 V. With increase of the treatment time to 10 minutes, the voltage drop rises to 600 V, the current waveform becomes a primary current pulse with a repetition rate of 4.5×10^4 pps, followed by repetitive secondary current pulses with lower amplitude, of which the repetition rate is 7×10^6 pps. When the treatment time was increased to 20 minutes, the repetitive secondary pulses were replaced by a long-tail current pulse of microsecond duration, with amplitude of 5 mA; the voltage drop increased to 800 V and the discharge repetition rate reduced to 2.8×10^4 pps. The significant changes to the observed current waveforms with increasing treatment time are indicative of a change of the discharge mode with increase of water conductivity.

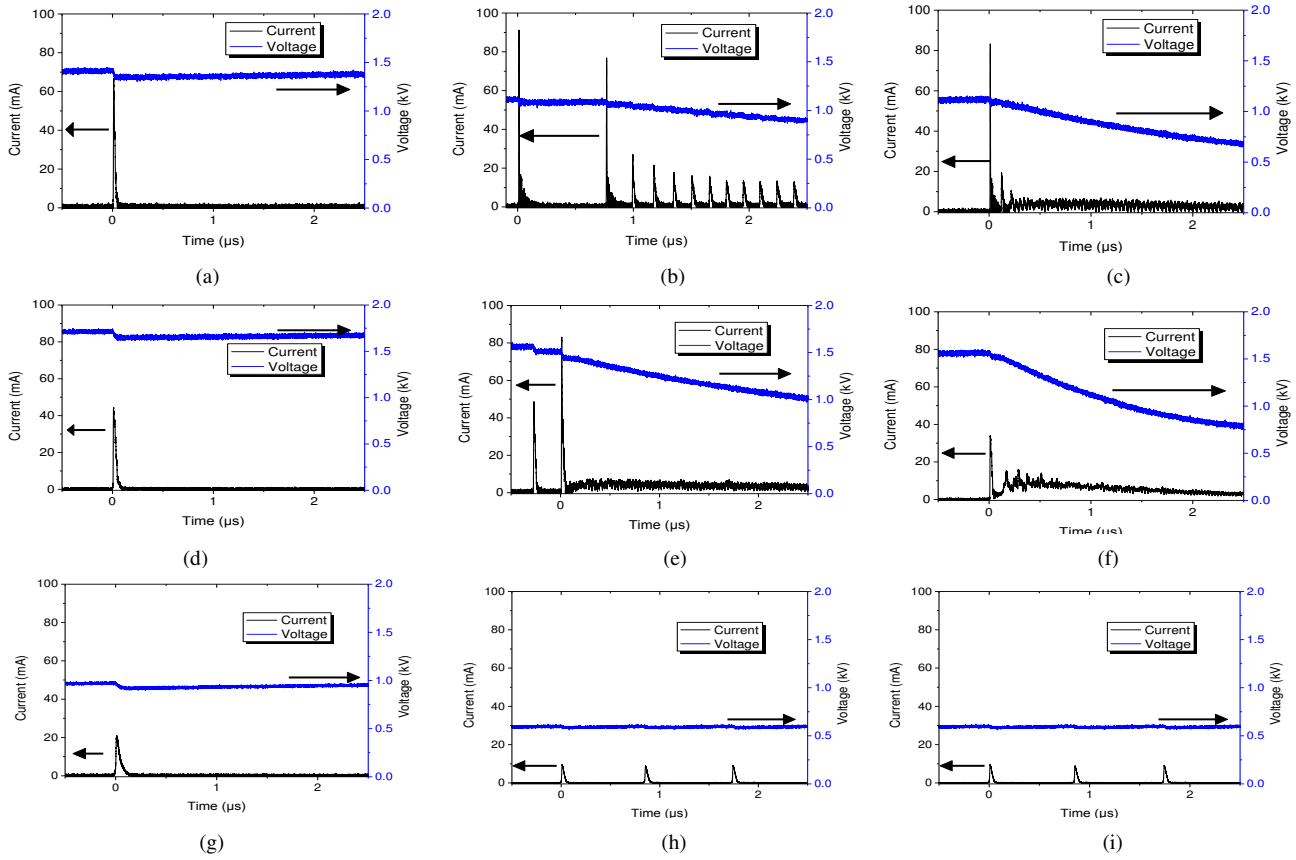

Fig. 2. Discharge current and voltage recorded: in air at (a) 0 minutes, (b) 10 minutes, and (c) 20 minutes; in nitrogen at (d) 0 minutes, (e) 10 minutes, and (f) 20 minutes; and in helium at (g) 0 minutes, (h) 10 minutes, and (i) 20 minutes.

The evolution of the discharge current waveform in nitrogen, as shown in Fig. 2(d), (e), and (f), is similar to the discharge in air. The amplitude of the microsecond-duration current pulse increased with treatment time, reaching 10 mA at 20 minutes. The discharge repetition rate dropped from 5×10^4 pps to 1.25×10^4 pps. The discharge current in air and nitrogen both show a short-duration current pulse, followed by a long-tail current pulse of ~2 μs duration. This can be explained by the increasing water conductivity, as shown in Fig. 3, which shows that the conductivity reached 145 μScm^{-1} in air and 134 μScm^{-1} in nitrogen, respectively, at 20 minutes. The water conductivity

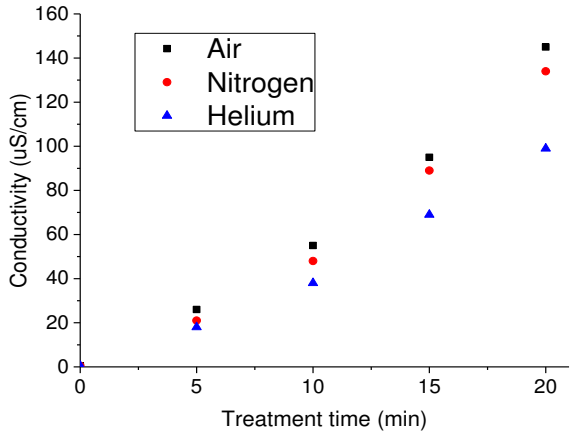

Fig. 3. measurement of water conductivity with treatment time.

increased with time, indicative of ion production in the water as a result of reactions occurring at the plasma-water interface. In air and nitrogen discharges, a certain amount of nitrate and nitrite are produced, causing the water conductivity to increase. The initial water conductivity was 0.5 μScm^{-1}, and the water acting as a dielectric barrier and presents capacitance characteristic. At the beginning of discharge, the voltage at the charge accumulation point increase to needle voltage, which inhibits the further development of the discharge. The charges release into water after discharge and the inter-duration between two discharge pulses presents the release time for charges in water. With increasing water conductivity, the water starts to present resistance characteristic, the resistance value decreasing results in a weaker inhibition effect. Thus, discharge can develop more fully and initiate secondary repetitive discharges in the channel. The repetition rate of the secondary current increased dramatically with increasing water conductivity, of which the water resistance further decreasing and a long-tail presents a more fully developed diffuse discharge after a nanosecond capacitive current.

The current behaviour in helium is different from that in air and nitrogen discharges. A short current pulse of duration 38 ns and magnitude 20 mA is superimposed on a d.c. charging current of 0.33 mA. The repetition rate increased from 5×10^5 pps to 1.25×10^6 pps from 0 to 10 minutes, and remained at 1.25×10^6 pps until 20 minutes, while the pulse current amplitude was reduced to 10 mA; the water conductivity

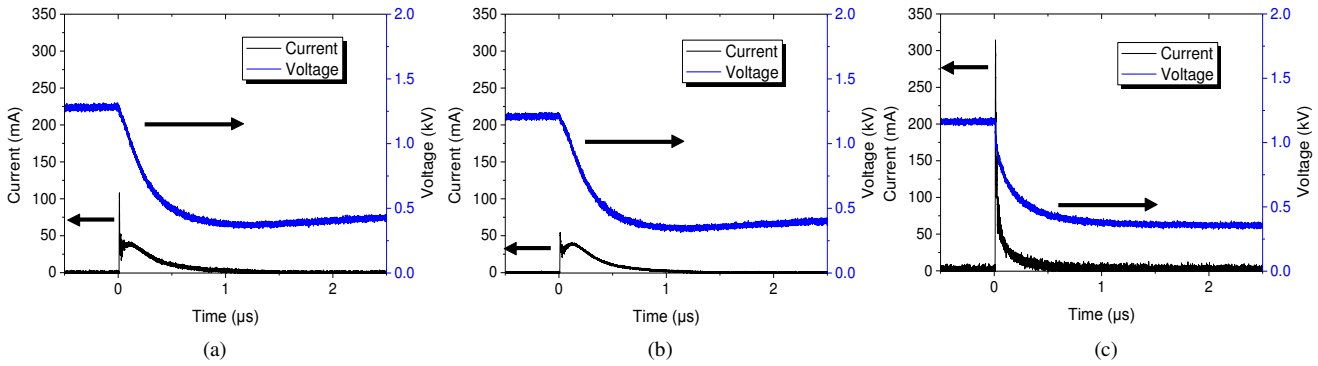

Fig. 4. Discharge voltage and current waveforms above NaOH solution for (a) air discharge, (b) nitrogen discharge and (c) helium discharge.

increased from the initial level of 0.5 μScm^{-1} to 99 μScm^{-1}. The d.c. voltage decreased from 1000 V to 630 V due to increase of the d.c. charging current from 0.33 mA to 0.4 mA. Although the concentration of H_2O_2 formed was higher in helium than in air and nitrogen (Section V), the water conductivity was the lowest, which is due to the low rate of electrolysis of H_2O_2. Z. Xiong [20] used a needle-plate metal electrode energized by a pulsed d.c. power supply and found that discharges in helium were characterised by a single current pulse, however, Trichel pulses were found in the discharges in oxygen and nitrogen. In the present work, using a water electrode, the dielectric barrier effect of water inhibits the development of an individual discharge, leading to repetitive secondary current pulses. P. Sunka [21] and B. Sun [22] investigated pulsed streamer corona discharges in water and found that the water conductivity plays an important role in discharge mode. The initial discharge in water is relatively weak, before the increased water conductivity leads to a diffuse discharge.

B. Discharge above 5-mM sodium-hydroxide solution

To compare with discharges above ultrapure water, high-conductivity solutions were used to investigate the current and voltage characteristics during the discharge. The 5-mM NaOH solutions used had a conductivity of 1250 μScm^{-1}, which was found to remain constant during the discharge. The discharge current has a tail component of amplitude 40 mA in air and nitrogen, following the nanosecond range capacitive current as shown in Fig. 4. The tails of the current waveforms in air and nitrogen discharges are similar to the results observed when using ultrapure water, suggesting that the long-tail current observed with increasing treatment time in ultrapure water is due to increasing water conductivity during the treatment. In a positive streamer discharge, positive ions at the streamer head move upon the solution surface, inducing the primary current pulse in the external circuit. A conductive channel is established to enable a follow-up diffuse discharge to develop when the solution conductivity is high enough, leading to the long-tail current pulse. In all of the gases investigated, the primary current pulse has duration of a few nanoseconds, followed by a tail current of duration ~0.5 μs in helium and ~1 μs in air and nitrogen. The voltage drop approached 1 kV in all cases. There is no obvious delay between the primary and secondary current in helium discharges; the current has higher amplitude of ~320 mA, compared to ~120 mA in air and ~70 mA in nitrogen, which is considered to be due to the much lower breakdown voltage of helium.

IV. Hydroxyl Radical Detection using Terephthalic Acid

The amount of OH formed in the solution was determined by using a terephthalic acid and fluorophotometry method. The conductivity of the initial solution was 1250 μScm^{-1}, and this remained constant during treatment. The results demonstrate that OH radical formation, in positive-polarity d.c. streamer discharges, was affected significantly by the gas type, as shown in Fig. 5. The OH radical concentration increased linearly during the 20-minute treatments, and the OH radical concentration reached 0.03 μmol, 0.06 μmol and 0.11 μmol in air, nitrogen and helium, respectively.

The concentration of OH radicals formed in helium was 3.7 times higher than that in air, and 1.8 times higher than that in nitrogen. In positive streamer discharges, the reaction of ions

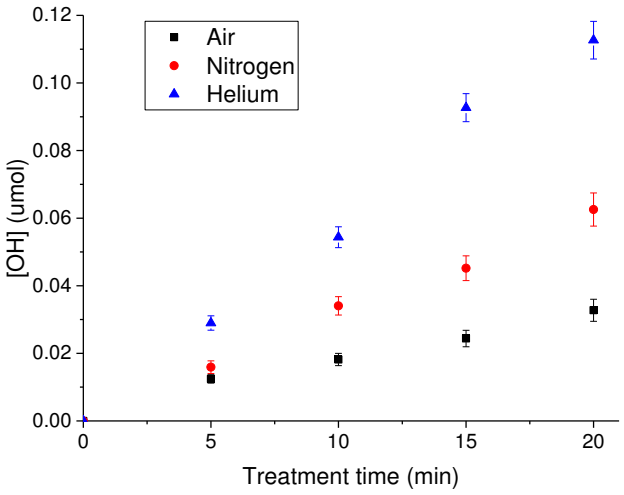

Fig. 5. OH formation in the terephthalic acid solution during air, nitrogen and helium discharge.

TABLE I
HYDROXYL RADICALS FORMATION REACTIONS

$N_2^+ + H_2O \rightarrow N_2 + H_2O^+$	(1)
$H_2O^+ + H_2O \rightarrow H_3O^+ + OH$	(2)
$N_2^* + H_2O \rightarrow OH + H + N_2$	(3)
$He + e \rightarrow He^+ + 2e$	(4)
$He^+ + H_2O \rightarrow He + H_2O^+$	(5)
$O_2 + e \rightarrow O_2^+ + 2e$	(6)
$O_2^+ + H_2O \rightarrow O_2 + H_2O^+$	(7)
$O_2 + e \rightarrow O + O + e$	(8)
$O + H_2O \rightarrow H_2O_2$	(9)
$H_2O + e \rightarrow H^- + OH$	(10)
$H_2O + e \rightarrow H + OH + e$	(11)
$H_2O + e \rightarrow H_2O^+ + 2e$	(12)
$H + O_2 \rightarrow HO_2$	(13)
$O + HO_2 \rightarrow OH + O_2$	(14)
$H + HO_2 \rightarrow 2\ OH$	(15)

with water is considered to be the major source of OH radicals. The energetic positive ions and excited-state molecules react with water to form OH radicals and ground-state gas molecules. The major chemical reactions occurring during the treatments in this study are summarized in Eqs. (1-15) in Table 1 [6, 23-27].

Oxygen atoms react with water molecules to form hydrogen peroxide, Eqs. (6-9). Energetic electrons react with gas-phase water molecules by collision and attachment to form OH radicals depending upon the energy level, Eqs. (10-12). Hydrogen atoms, the product of direct water molecule collisional separation, can further react with oxygen and HO_2, leading to OH radical formation, Eqs. (13-15).

V. HYDROXYL RADICAL DETECTION USING TITANIUM (IV) AND TERT-BUTANOL

There are various reactions leading to the formation of hydrogen peroxide at the plasma-water interface. A major reaction path is through the dimerization of OH radicals, as shown in Eq. (16). To determine the amount of OH radicals formed, hydrogen peroxide was measured with Tert-butanol added to the solution, which is an effective OH radical scavenger as described in Eq. (17) [7], to terminate OH radical dimerization. By measuring the difference of hydrogen peroxide formation with and without the addition of Tert-butanol to the solution, it is possible to determine the amount of hydroxyl radicals formed.

$$2\ OH \rightarrow H_2O_2 \quad (16)$$

$$OH + CH_3C(CH_3)_2OH \rightarrow CH_2C(CH_3)_2OH + H_2O \quad (17)$$

The addition of Tert-butanol does not change the solution conductivity. Spectrophotometric determination of H_2O_2 by using potassium titanium (IV) oxalate was employed to determine the formation of H_2O_2. Titanium (IV) - peroxide complex, the product of H_2O_2 reacting with titanium (IV), has a yellow-orange colour, with an absorption peak at λ_{max}=396 nm.

A. Discharge above 5-mM sodium-hydroxide solution

In order to make comparisons with OH radical detection using the terephthalic acid and fluorophotometry method (Section IV), a 5-mM NaOH solution was used in the treatment. Without the Tert-butanol added to the solution, the amount of H_2O_2 detected increased linearly with time up to 20 minutes, and reached 0.78 µmol, 2.76 µmol and 3.31 µmol in air, nitrogen and helium, respectively, as shown in Fig. 6(a). In comparison, when the Tert-butanol was added to the solution, the amount of H_2O_2 detected after 20 minutes treatment was reduced to 0.75 µmol, 0.71 µmol and 1.04 µmol in air, nitrogen and helium, respectively. It can be calculated that 4%, 74% and 68% of the H_2O_2 formation in air, nitrogen and helium, respectively, was obtained from OH radicals; the corresponding amount of OH radicals is 0.06 µmol, 4.1 µmol and 4.54 µmol.

OH radicals played an important role in H_2O_2 formation under nitrogen and helium, but had very limited contribution to H_2O_2 formation in air. The results suggest that the major reaction leading to H_2O_2 formation in nitrogen and helium is OH dimerization. In air, the possible paths are hydrogen atoms reacting with HO_2, and HO_2 dimerization. HO_2 can lead to H_2O_2 formation by reactions in water vapour, as shown in Eqs. (18-19). Reactions of excited oxygen molecules and atoms with water may lead to H_2O_2 formation in the solution in an air discharge. Other than that, electron attachment to oxygen molecules can also lead to H_2O_2 formation by the reactions shown in Eqs. (13, 20-24) [6, 24-29].

$$H + HO_2 \rightarrow H_2O_2 \quad (18)$$

$$2HO_2 \rightarrow H_2O_2 + O_2 \quad (19)$$

$$O_2 + e \rightarrow O_2^- \quad (20)$$

$$O_2^- + H^+ \leftrightarrow HO_2 \quad (21)$$

$$HO_2 + e \rightarrow HO_2^- \quad (22)$$

$$HO_2^- + H^+ \rightarrow H_2O_2 \quad (23)$$

$$HO_2 + H \rightarrow H_2O_2 \quad (24)$$

In comparison to the OH radical detection results using the TA method, the results obtained using Tert-butanol are 2 times, 68 times and 41 times higher in air, nitrogen and helium, respectively. The significant difference suggests that the formation of OH radicals at the interface was inhibited in the solutions consisting of terephthalic acid and NaOH.

B. Discharge above ultrapure water

Due to the difference in discharge mode above ultrapure water, H_2O_2 formation using ultrapure water was also measured. In Fig. 6(b), the amount of H_2O_2 increased almost linearly with time and reached 2.15 µmol, 5.24 µmol and 9.94 µmol in air, nitrogen and helium, respectively, after 20 minutes of treatment,

which is 2.8 times, 1.9 times and 3.0 times higher compared to

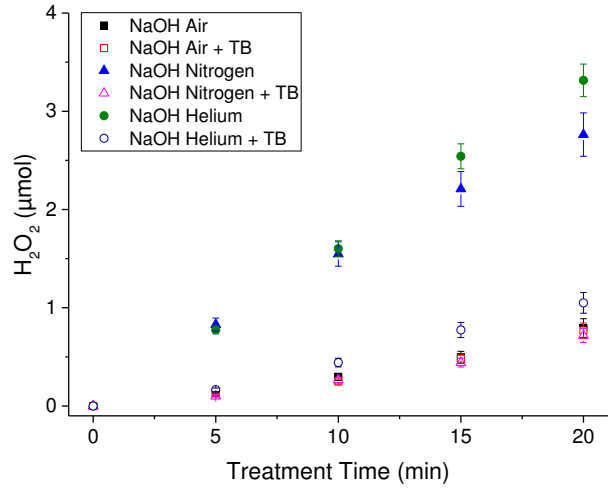

(a) H_2O_2 measured in NaOH solution.

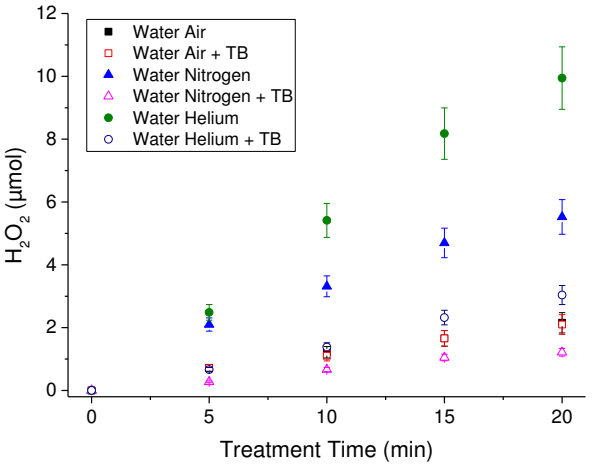

(b) H_2O_2 measured in ultrapure-water solution.

Fig. 6. H_2O_2 production measured from discharge above solution of (a) NaOH and (b) ultrapure water.

the results obtained in the discharge above NaOH solution. The difference may be caused by different discharge modes in NaOH solution and ultrapure water. The NaOH solution itself may inhibit the formation of hydroxyl radicals at the interface reactions; this requires further investigation.

H_2O_2 formation was reduced when the OH scavenger Tert-butanol was added to the solution. Only 2 µmol, 1.2 µmol and 3 µmol of H_2O_2 were detected after 20 minutes treatment in air, nitrogen and helium, respectively. It can be calculated that 7% (air), 78% (nitrogen) and 70% (helium) of the H_2O_2 detected was formed by OH radicals, as shown in Fig. 6(b). The remaining 22% and 30% of the H_2O_2 formation in nitrogen and helium, respectively, may be due to reactions occurring in water vapour to form H_2O_2, subsequently dissolved in the solution during treatment.

Similar to the results obtained using NaOH solution, little effect on H_2O_2 formation was observed in air by adding Tert-butanol to the solution. Fig. 7 plots the reaction paths for OH radical and H_2O_2 formation in air, nitrogen and helium discharges. Hydroxyl radical dimerization, as shown in Eq. (16), is the major source of hydrogen peroxide formation in nitrogen and helium discharges. The discharge in helium has the highest formation of OH and H_2O_2 whether using NaOH solution or ultrapure water.

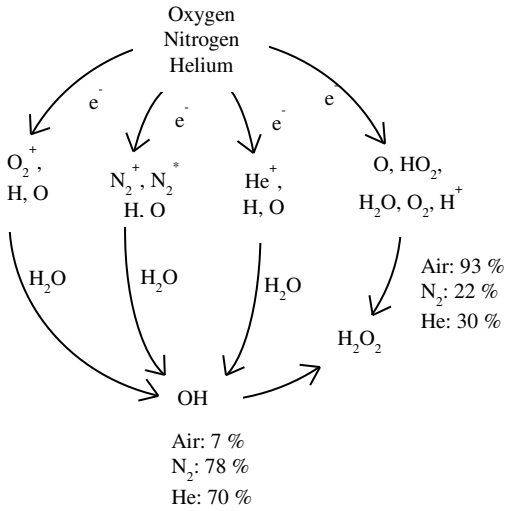

Fig. 7. Diagram demonstrating OH radical and H_2O_2 formation paths in discharge above ultrapure water.

VI. Conclusions

The conductivity of ultrapure water increased with treatment time as a result of ion formation in the water through plasma-water interfacial reactions. The solution conductivity plays an important role in determining the discharge mode. The amplitude of the tail associated with the observed current pulses started to increase when the water conductivity rose to ~30 μScm^{-1}, reaching 5 mA at 145 μScm^{-1} in air discharges, indicating a transition to the diffuse discharge mode. It was identified that 4%, 74%, and 68% of the H_2O_2 formation using NaOH solution was via OH dimerization in air, nitrogen and helium discharges, respectively; the corresponding contributions in ultrapure water were 7%, 78% and 70%. OH radical dimerization is the major path for H_2O_2 formation in nitrogen and helium discharges. Discharges in helium yield the highest OH and H_2O_2 formation. The concentrations of OH radicals detected using the fluorophotometry and TA method were much lower than those determined using the Tert-butanol method; the terephthalic acid and NaOH solution may inhibit the formation of hydroxyl radicals.

References

[1] O. Lesage. (2013, Oct). Treatment of 4-chlorobenzoic acid by plasma-based advanced oxidation processes. Chemical Engineering and Processing: Process Intensification. 72, pp. 82-89

[2] M. Nageeb Rashed. (2013, Jan). Organic Pollutants - Monitoring, Risk and Treatment. (1st) [Online]. Aviliable: http://dx.doi.org/10.5772/55953

[3] Y.S. Mok. (2007). Application of dielectric barrier discharge reactor immersed in wastewater to the oxidative degradation of organic contaminant. Plasma Chemistry and Plasma Processing. 27, pp. 51–64

[4] K. Kutschera. (2009). Photo-initiated oxidation of geosmin and 2-methylisoborneol by irradiation with 254 nm and 185 nm UV light. Water Research. Volume (43), pp. 2224–2232
[5] L.O. de B. Benetolia. (2012, Oct). Pyrite-enhanced methylene blue degradation in non-thermal plasma water treatment reactor. Journal of Hazardous Materials. 237– 238, pp. 55– 62
[6] B.R. Locke. (2011, April). Review of the methods to form hydrogen peroxide in electrical discharge plasma with liquid water. Plasma Sources Science and Technology. 20, 034006
[7] M. Ismail. (2013, Jul). Advanced oxidation for the treatment of chlorpyrifos in aqueous solution. Chemosphere. 93, pp. 645–651
[8] P. Andre. (2001, Dec). Experimental study of discharge with liquid non-metallic (tap-water) electrodes in air at atmospheric pressure. Journal of Physics D: Applied Physics. 34, pp. 3456-3465
[9] X. Lu. (2003, Feb), Ignition phase and steady-state structures of a non-thermal air plasma. Journal of Physics D: Applied Physics. 36, pp. 661-665
[10] X. Lu. (2003, Oct). Optical and electrical diagnostics of a non-equilibrium air plasma. Journal of Physics D: Applied Physics. 36, pp. 2662-2666
[11] S. Kanazawa (2011). Observation of OH radicals produced by pulsed discharges on the surface of a liquid. Plasma Sources Science and Technology. 20(3) 034010
[12] S. Kanazawa (2012). Measurement of OH Radicals in Aqueous Solution Produced by Atmospheric-pressure LF Plasma Jet. Electrostatics Society of America. N(3)
[13] S.L. Li, S. Hu (2012). Formation of hydroxyl radicals and hydrogen peroxide by a novel nanosecond pulsed plasma power in water. IEEE Transactions on Plasma Science. 40, pp. 63-67
[14] B. Bektasoglu. (2008, Jul). Hydroxyl radical detection with a salicylate probe using modified CUPRAC spectrophotometry and HPLC. The International Journal of Pure and Applied Analytical Chemistry, 77. PP. 90–97
[15] R.W. Matthews. (1980, Jul). The radiation chemistry of aqueous sodium terephthalate solutions. Radiation Research Society. [Online]. 83(1) pp. 27-41. Aviliable: http://www.jstor.org/stable/3575256
[16] M. Tahara. (2014, April). Detection of free radicals produced by a pulsed electrohydraulic discharge using electron spin resonance. Journal of Electrostatics. 72, pp. 222-227
[17] R.M. Sellers. (1980, Oct). Spectrophotometric determination of hydrogen peroxide using potassium titanium(IV) oxalate. Analyst. [Online]. 105, pp. 950-954. Aviliable: http://pubs.rsc.org/en/content/articlepdf/1980/an/an9800500950
[18] J. Ma. (2000, Jan). Degradation of atrazine by manganese-catalysed ozonation influence of radical scavengers. Water Research. 34(15), pp. 3822-3828
[19] C. Tizaoui. (2009, Jul). Effect of the radical scavenger t-butanol on gas–liquid mass transfer. Chemical Engineering Science. 64, pp. 4375-4382
[20] Z. Xiong. (2013, Jul), On the electrical characteristic of atmospheric pressure air/He/O_2/ N_2/Ar plasma needle. IEEE transactions on plasma science, 41(7), pp. 1746-1750
[21] P. Sunka (1999, Jan). Generation of chemically active species by electrical discharges in water. Plasma Sources Science and Technology. 8, pp. 258–65
[22] B. Sun (1997). Optical study of active species produced by a pulsed streamer corona discharge in water. Journal of Electrostatics. 39, pp. 189–202
[23] A. Fridman, "Elementary Plasma-Chemical Reactions," in Plasma chemistry, 1st ed., New York: Cambridge University Press, 2008, pp. 56-133
[24] T. Verreycken. (2010, Jun). Spectroscopic study of an atmospheric pressure dc glow discharge with a water electrode in atomic and molecular gases. Plasma Sources Science and Technology. 19(4), 045004
[25] P. Bruggeman. (2010, Jul). On OH production in water containing atmospheric pressure plasmas. Plasma Sources Science and Technology. 19(4), 045025
[26] I.A. Soloshenko. (2009, Sept). Effect of water adding on kinetics of barrier discharge in air. Plasma Sources Science and Technology. 18(4), 045019
[27] A.A. Joshi. (1994, Sept). Formation of hydroxyl radicals, hydrogen peroxide and aqueous electrons by pulsed streamer corona discharge in aqueous solution. Journal of Hazardous Materials. 41(1), pp. 3-30
[28] M.J. Kirkpatrick (2005, May) Hydrogen, oxygen, and hydrogen peroxide formation in aqueous phase pulsed corona electrical discharge. Industrial and Engineering Chemistry Research. 44(12), pp. 4243-4248
[29] R. Xiong. (2012, Jan). Hydrogen Peroxide Generation by DC and Pulsed Underwater Discharge in Air Bubbles. Journal of Advanced Oxidation Technologies. 15, pp. 197-204

Yiyi Zhao received the B.Eng. degree in Electronic and Electrical Engineering from the University of Strathclyde (Glasgow, UK) in 2012. From 2012, she has been working towards the Ph.D. degree in the High Voltage Technology group in the Department of Electronic and Electrical Engineering at the University of Strathclyde. Her current research interest includes non-thermal plasma discharge applications in water modification, purification and disinfection.

Tao Wang received the B.Eng and M.Sc degrees from Northeast China Dianli University in 1993 and 1996 respectively, and the Ph.D. degree from the University of Strathclyde (Glasgow, UK) in 2005. He then joined the Newland Group as a research fellow developing industrial ozone generator. He joined the Department of Electronic and Electrical Engineering of University of Strathclyde as a lecturer in 2010. His research interests include non-thermal plasma and their applications in gas synthesis, plasma water interactions, water purification and advanced oxidation process.

Scott J. MacGregor (M'95-SM'14) received the B.Sc. and Ph.D. degrees from the University of Strathclyde, Glasgow, U.K., in 1982 and 1986, respectively. He became a Pulsed Power Research Fellow in 1986 and a Lecturer in pulsed-power technology in 1989. In 1994, he became a Senior Lecturer, with a promotion to Reader and Professor of High Voltage Engineering, in 1999 and 2001, respectively. In 2006 and 2010 he became the Head of the Department of Electronic and Electrical Engineering and Executive Dean of the Faculty of Engineering, and has been the Vice-Principal of the University of Strathclyde since 2014. Professor MacGregor was the recipient of the 2013 IEEE Peter Haas Award, and he was appointed as an Associated Editor of the IEEE Transitions on Dielectrics and Electrical Insulation in 2015. His research interests include high-voltage pulse generation, high-frequency diagnostics, high-power repetitive switching, high-speed switching, electronic methods for food pasteurization and sterilization, generation of high-power ultrasound (HPU), plasma channel drilling, pulsed-plasma cleaning of pipes, and stimulation of oil wells with HPU.

Qing Chun Ren is currently a senior research fellow in the Department of Electronic and Electrical Engineering at the University of Strathclyde. He has been working on ecological environment research since his graduation from Tsinghua University (Beijing, China). His research interests include desalination techniques, nanofiber filters, treatment of high salinity and high organic content industrial wastewater, zero liquid discharge wastewater treatment in cities and industrial estates.

Mark P. Wilson (M'10) was born in Stranraer, Scotland, in 1982. He received the B.Eng. (with honours), M.Phil., and Ph.D. degrees in electronic and electrical engineering from the University of Strathclyde, Glasgow, U.K., in 2004, 2007, and 2011, respectively. He is presently working as a Teaching Associate at the University of Strathclyde, where he continues to investigate surface flashover of solids immersed in insulating oil. Mark is a member of the IEEE Nuclear and Plasma Sciences Society, from whom he received a Graduate Scholarship Award in 2011, the IEEE Dielectrics and Electrical Insulation Society, and the IET.

Igor V. Timoshkin (M'07-SM'14) received a degree in M.Phys from Moscow State University, Moscow, Russia, in 1992, and the Diploma and Ph.D. degrees from the Imperial College of Science, Technology and Medicine, London, U.K., in 2001. He was a Researcher with Moscow State Agro-Engineering University, Moscow, and with the Institute for High Temperatures, Russian Academy of Sciences, Moscow. He moved to ICSTM, London, in 1997. He joined the Department of Electronic and Electrical Engineering of the University of Strathclyde (Glasgow, UK) in 2001 where he became a Reader in 2016. His current research interests include properties of solid and liquid dielectric materials, electronics of plasma discharges in condensed media, practical applications of electro-hydraulic and high-power ultrasound pulses, bio-dielectrics, and effects of electromagnetic fields on biological objects.